Gate-tunable THz detector based on a quantum Hall device

C Stellmach[1], A Hirsch[1], N G Kalugin[1], G Hein[2], B E Sağol[1,2] and G Nachtwei[1]

[1] Institut für Technische Physik, TU-Braunschweig, Mendelssohnstraße 2,
D-38106 Braunschweig, Germany
[2] Physikalisch-Technische Bundesanstalt, Bundesallee 100, D-38116 Braunschweig,
Germany

E-mail: c.stellmach@tu-bs.de

Abstract
Recent investigations showed that the THz photoresponse of quantum Hall
systems (QHS) is a complex combination of different mechanisms. In this
work, we separate these parts by varying the electron concentration and the
source–drain current. For our photoconductivity measurements, we used a
pulsed p-Ge cyclotron laser as a monochromatic THz radiation source and
changed the magnetic field, the source–drain current and the electron
concentration (via a backgate) of the QH sample. The spectral resolution of
the QHS was found to improve with increasing values of the source–drain
current up to the breakdown of the QH effect.

Measurements of the far-infrared (FIR) photoconductivity of
quantum Hall systems (QHS) [1] are interesting with respect to
the application of QHS for sensitive and tunable FIR detectors
[2, 3], since QHS develop Landau gaps of the order of
$E_g = \hbar\omega_c = 10$ meV, corresponding to waves of about
100 μm length. Further, the basic mechanisms of the
photoconductivity which determine the photoresponse (PR)
of QHS are still the subject of discussion. Whereas most of
the previous works were focussed on the bolometric change
of the longitudinal resistance of QHS [2, 3], we confirmed
a far more complex behaviour: bolometric and cyclotron-
resonant contributions to longitudinal (see also [4]) and also
Hall-related parts of the photosignal [5, 6].

In this study, we present measurements of the
photoconductivity of QHS using FIR laser radiation (THz
radiation). The radiation source is a p-type Ge light-
hole cyclotron-resonance laser (pulsed operation, see also
[7]). By applying a backgate voltage, we investigate the
photoconductivity as a function of the carrier concentration
to separate the different contributions of the FIR-PR.
We changed the source–drain current I_{SD} and found the
spectral resolution of the detectors improves with I_{SD} up
to the critical current for the breakdown of the QH effect
(QHE).

The laser system and the QH sample are jointly mounted
on one measuring insert immersed in liquid helium at 4 K. The
laser radiation is guided via a waveguide to the QH sample (see
figure 1(*a*)).

The QH sample used for this study is a meander, patterned
photolithographically from GaAs/GaAlAs heterostructures
(see inset of figure 2). The meander geometry is preferable
for photoconductivity measurements due to the relatively large
area and the favourable length-to-width ratio [2, 3]. The wafer
from which the sample is patterned has an electron density of
2×10^{11} cm^{-2} and mobility of 600 000 cm^2 V^{-1} s^{-1}.

The laser crystal in use is p-doped with a density of $p \approx$
2×10^{14} cm^{-3}. Al-electrodes are located at the two parallel
sides to apply the electric field. Such a laser system emits FIR
radiation in the wavelength range around 100 μm. The optical
pulse power is approximately 1 W.

The laser is operated by means of electrical pumping
with pulses of peak voltages of 1–2 kV at currents of about
50 A through the Ge crystal. Stimulated emission is only
possible in a certain 'window' of the $\boldsymbol{E} \times \boldsymbol{B}$ area. This is due
to the function principle of the laser (for further details see
[7]).

Figure 1(*b*) shows the photosignal of the QH sample as a
function of $|\boldsymbol{E}|$ in units of V $(0.5$ cm$)^{-1}$ and $|\boldsymbol{B}|$. The photon
energy changes with the magnetic field at the laser crystal
$(\hbar\omega_c = \hbar eB/m^*)$. Thus, the signal is a function of both the
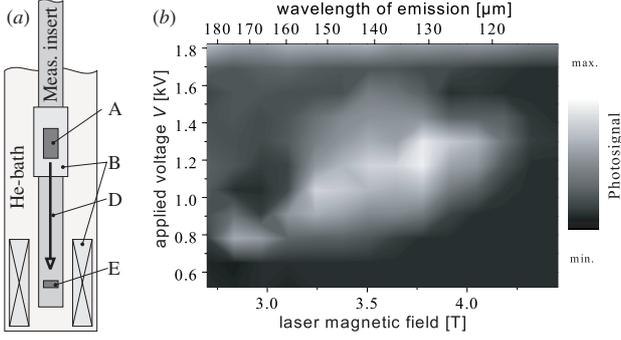spectral emission of the laser and the spectral sensitivity of the
QH detector.

Figure 1. (*a*) Scheme of the measurement setup with two magnet coils (B), one for the laser crystal (A) and one for the QH sample (E). The radiation is guided via a waveguide (D) to the QH sample. (*b*) Photosignal of the QH sample ($I_{SD} = 15\ \mu$A, $B = 4.3$ T) as a function of the electric and magnetic fields at the laser crystal ('operational window' of the laser).
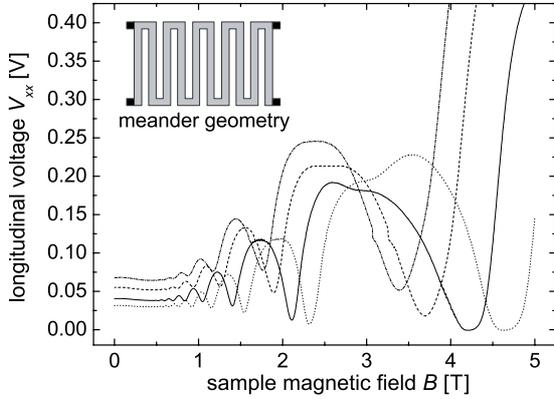

Figure 2. Magnetoresistance traces of the detector for different backgate voltages from: $V_{Gate} = -250$ V ($\cdots\cdots$), -150 V (- - - -), 0 V (——), $+150$ V ($\cdots\cdots$). The minima near 4 T correspond to filling factor $\nu = 2$. Inset: meander geometry (schematic). The sample used has 100 μm channel width, 6 cm channel length, 30 channel sequences.

To check the time resolution of the laser system, we realized a pumping pulse source with a switching module based on field-effect transistors (FET), capable of generating pulses of variable length t_{el} and steep pulse flanks ($t_{el} = 0.3\ \mu$s to 50 μs, dV/d$t \approx 150$ V ns^{-1}). For $t_{el} < 2\ \mu$s the emitted intensity drops markedly. The extrapolation of the data yields a minimum duration of the optical pulse of about 0.1 μs.

Besides the detection of the laser emission by using QH detectors, we also studied the laser pulses by means of a hot-electron bolometer (HEB) [8] and found an optical pulse duration of about 500 ns for electric pumping pulses of a fixed duration of $t_{el} \approx 5\ \mu$s.

Our recent works showed that the phoconductivity in QHS is a complex interaction of different mechanisms [5, 6]. From time-resolved measurements, we deduced that the PR is composed as follows.

First, bolometric and cyclotron-resonant contributions are distinguishable. The bolometric part (BO) is due to non-resonant excitations and dominates at magnetic fields near the QH plateaux. Cyclotron resonance (CR) occurs for the

coincidence of the Landau level splitting with the photon energy.

Second, by reversing the magnetic field direction, we were able to separate alterations of the longitudinal resistance (ΔR_{xx}) from changes of the Hall signal due to changes of the Hall resistance (ΔR_{xy}) and FIR-induced Hall currents I_{Hall}^{photo}. Thus, we obtain for the entire photosignal:

$$\Delta V_x = \left(\Delta R_{xx}^{BO} + \Delta R_{xx}^{CR}\right) I_{SD}$$
$$+ \left(R_{xy} + \Delta R_{xy}^{BO} + \Delta R_{xy}^{CR}\right) I_{Hall}^{photo}. \quad (1)$$

As only the Hall part of the signal depends on the direction of the magnetic field, the longitudinal and Hall-related contributions can be deduced from the result of two measurements at different magnetic field directions.

There are also parts of the photoresponse with remarkably long decay times ($t \geqslant 280\ \mu$s). These parts are only longitudinal ones (for further details see [5, 6]).

In the following passage, we report on our measurements of the spectral resolution of the FIR-QH detectors as a response to the laser radiation. QHS are very sensitive for FIR radiation and are therefore very suitable as detectors for wavelengths around 100 μm. To tune the FIR-QH detectors, a controllable electron density n_s is desirable. The adjustment of n_s is realized by a backgate. This requires rather high backgate voltages of V_{Gate} between -250 V and $+400$ V to reach noticeable changes of the electron density, as the voltage drops over the entire substrate thickness. Within the gate voltage range mentioned, we obtained a shift of the SdH minimum at the filling factor $\nu = 2$ of approximately 0.3 T/100 V (see figure 2). This corresponds to a change of the electron density with the gate voltage of dn_s/d$V_{Gate} \approx 1 \times 10^{12}$ V^{-1} m^{-2}.

By variation of both the electron density n_s and the sample current I_{SD}, a separation of the cyclotron-resonant contribution from the bolometric one was possible. The aim of this study was to determine the spectral resolution of the FIR-QH detectors. In the resonant mode, the cyclotron energy $\hbar\omega_c$ of the detector has to be in coincidence with the incident photon energy $\hbar\omega_{phot}$. This can in principle be achieved by tuning the magnetic field to $\hbar eB/m^* = \hbar\omega_{phot}$. However, as the sensitivity of the detector is also a strong function of the filling factor (or the relative position of the Fermi energy with respect to the Landau levels), the carrier density n_s has to be adjusted correspondingly while tuning the magnetic field of the detector to cyclotron resonance.

For this, the magnetic field dependence of the photosignal was measured at a fixed delay time (approximately 5 μs) after the onset flank of the laser pulse for a fixed laser wavelength and various electron densities n_s. These measurements were performed for several sample currents I_{SD}.

The upper part of figure 3(*a*) shows the photosignal of the FIR-QH detector for a sample current $I_{SD} = 34\ \mu$A, which is near the critical current of the breakdown of the QHE. The values of the gate voltage are indicated near the curves. In the lower part of figure 3(*a*), the longitudinal resistance of the sample as a function of the magnetic field near the filling factor $\nu = 2$ is shown for various electron densities n_s to illustrate the filling factor dependence of the photosignal traces in the upper part of figure 3(*a*). Figure 3(*b*) shows the spectral resolution of the detector by plotting the maxima of the photosignal traces for a fixed laser line at $\hbar\omega_{phot} = 8.11$ meV and for different
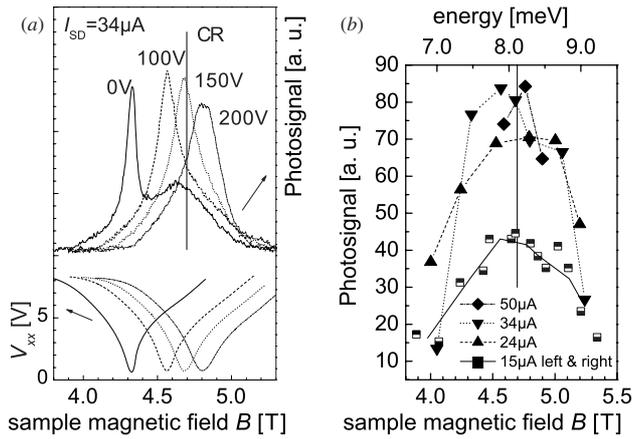
Figure 3. (*a*) Photoresponse (upper part) and corresponding magnetoresistance (lower part) curves as a function of *B* for different backgate voltages (denoted against the curves). The bolometric and resonant signals are distinguishable (see $V_{Gate} = 0$ V). (*b*) Spectral resolution (fixed laser line at 8.11 meV) of the detector at different sample currents (the points are the maxima of the photosignal traces, 15 μA: PR shows double peak, half-filled squares stand for left and right maxima). The currents (values given in the diagram) vary from below to beyond the critical breakdown value $I_c \approx 30$ μA.

sample currents I_{SD}. All points correspond to a constant filling factor, realized by adjusting n_s via the backgate voltage V_{Gate} to the shift of the magnetic field.

From our measurements, we observe that the spectral resolution of the FIR-QH detector is a function of the sample current. At currents lower than the critical current of the breakdown of the QHE, the bolometric part of the signal dominates, and the spectral resolution is relatively low. At sample currents reaching the critical value of the QH breakdown, the bolometric and the cyclotron-resonant part are separable. At sample currents exceeding the critical current, the cyclotron-resonant part dominates. In general, the spectral resolution of the FIR-QH detector improves with increasing sample current.

To summarize, we have generated FIR laser radiation in the wavelength range from 120 μm $\leqslant \lambda \leqslant$ 170 μm by means of a pulsed p-Ge laser with pulse length from 300 ns up to some microseconds. The radiation was detected by sensitive QH detectors, which show a complex photoresponse consisting of bolometric and cyclotron-resonant contributions to longitudinal and Hall-related signal parts. The spectral resolution of the FIR-QH detector depends on the sample current. In general, the spectral resolution of the FIR-QH detector improves with increasing sample current. At currents lower than the critical current of the breakdown of the QHE, the spectral resolution is relatively low while the bolometric part of the signal dominates. At sample currents near the critical value of the QH breakdown, the bolometric and the cyclotron-resonant parts are separable. At sample currents exceeding the critical current, the cyclotron-resonant part dominates.

Acknowledgments

References

[1] von Klitzing K, Dorda G and Pepper M 1980 *Phys. Rev. Lett.* **45** 494
[2] Kawano Y, Hisanaga Y, Takenouchi H and Komiyama S 2001 *J. Appl. Phys.* **89** 4037
[3] Hirakawa K, Yamanaka K, Kawaguchi Y, Endo M, Saeki M and Komiyama S 2001 *Phys. Rev.* B **63** 085320
[4] Stein D, Ebert G, von Klitzing K and Weimann G 1984 *Surf. Sci.* **142** 406
  Stein D 1983 *Diploma Thesis* TU-München
[5] Kalugin N G, Vasilyev Yu B, Suchalkin S D, Nachtwei G, Sağol B E and Eberl K 2002 *Phys. Rev.* B **66** 085308
[6] Kalugin N G, Nachtwei G, Vasilyev Yu B, Suchalkin S D and Eberl K 2002 *Appl. Phys. Lett.* **81** 382
[7] Ivanov Yu L and Vasilyev Yu B 1983 *Sov. Tech. Phys. Lett.* **9** 264
  Unterrainer K, Kremser C, Gornik E and Ivanov Yu L 1989 *Solid-State Electron.* **32** 1527
[8] Semenov A D, Hübers H-W, Schubert J, Gol'tsman G N, Elantiev A I, Voronov B M and Gershenzon E M 2000 *J. Appl. Phys.* **88** 6758